Audio Engineering Society
Convention Paper
Presented at the 112th Convention
2002 May 10–13 Munich, Germany

A New Set of Fifth and Sixth-Order Vented-Box Loudspeaker System Alignments using a Loudspeaker-Enclosure Matching Filter: Part II

Tim J. Mellow

Nokia Product Creation Centre, Farnborough, Hants GU14 0NG, England
Correspondence should be addressed to tim.mellow@nokia.com

ABSTRACT

In Part I, a new vented-box loudspeaker system was introduced that uses a Loudspeaker Enclosure Matching Filter to provide a pre-determined frequency-response shape over a fairly wide and continuous range of box volumes. The Butterworth shape was used as an example as this is fairly well known. In this part, alternative frequency response shapes are discussed. Also, some other remaining topics are addressed such as box losses and diaphragm displacement.

0 INTRODUCTION

The main question that this paper attempts to answer is: Which standard frequency-response shapes are most suitable for use with a vented-box loudspeaker system with a Loudspeaker Enclosure Matching Filter (LEMF)? The parameters we wish to keep within reasonable bounds are diaphragm excursion (to limit distortion), box volume and power lift (extra power drawn at low frequencies due to the filter response). Firstly, alignment tables are derived for a range of standard frequency-response shapes using a vented -box system with an isolated high-pass filter. These are supplemented with plots of amplitude and diaphragm displacement. This is then repeated with a non-isolated filter. In this way, the two extremes of the range of LEMF alignments are fully represented. We can now choose which response shapes are most suitable and generate LEMF alignments for them.

The alignments listed here are all lossy with a Q_L value of 7, except for the 6th-order LEMF alignments, which are virtually impossible to solve with box losses included in the model. However, suitable correction factors can be extrapolated from the lossy 6th-order isolated and non-isolated alignments. Although the enclosure loss is theoretically frequency-dependent, its effect is only really significant over a fairly narrow frequency range around the box resonance f_B. Therefore, the approximation that results from the use of a pure resistor as a model for this loss should be fairly good.

The range of frequency-response shapes presented is fairly small because the need for multiple sub-Butterworth and Chebyshev alignments is largely eliminated by the LEMF. These were originally employed as a means of increasing the usable range of box volumes and an exhaustive range of alignments for a vented-box system with an isolated filter has previously been derived by Bywater and Wiebell [1].

1 MODEL OF A DRIVER IN A LOSSY VENTED BOX

A simplified equivalent electrical circuit of the driver in a vented box is shown in Fig. 1.

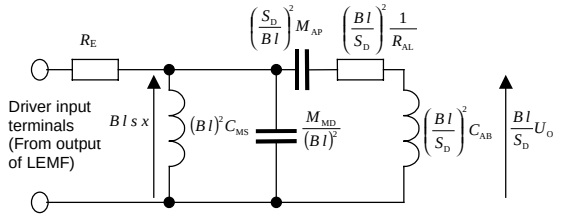

Fig. 1. Equivalent electrical circuit of a driver in a lossy vented box

The driver mechanical resistance and coil inductance is ignored. As suggested by Small [1], the various enclosure losses can be lumped together with the acoustic leakage resistance R_{AL}. The combined Q of the box resonance is given by

$$Q_L = R_{AL}\sqrt{\frac{C_{AB}}{M_{AP}}} \tag{1}$$

According to Small, Q_L values typically range from 5 to 20, so a nominal value of 7 is assumed from here onwards. The acoustic mass of the air load is included with the diaphragm mass M_{MD} and also with the end correction of the vent mass M_{AP}. The sound pressure $p(r)$ at a distance r in free space for a given output volume velocity U_O is given by

$$p(r) = \frac{\rho_0\, s\, U_O}{4\pi r} \tag{2}$$

2 6TH-ORDER FREQUENCY RESPONSE SHAPES

A generic 6th-order high-pass system transfer-function that relates the sound pressure $p(r)$ at a distance r in free space for a given voltage e_{in} at the input of the LEMF is given by

$$p(r) = \frac{\left(\frac{A\,\rho_0\, S_D\, Bl}{4\pi r\, M_{MD}\,(R_E + R_S)}\right) s^6 e_{in}}{\left(s^2 + \frac{\omega_1}{Q_1}s + \omega_1^2\right)\left(s^2 + \frac{\omega_2}{Q_2}s + \omega_2^2\right)\left(s^2 + \frac{\omega_3}{Q_3}s + \omega_3^2\right)} \tag{3}$$

$$= \frac{\left(\frac{A\,\rho_0\, S_D\, Bl}{4\pi r\, M_{MD}\,(R_E + R_S)}\right) s^6\, e_{in}}{s^6 + k_5\, s^5 + k_4\, s^4 + k_3\, s^3 + k_2\, s^2 + k_1\, s + k_0} \tag{4}$$

where

ρ_0 is the density of air (=1.18 kg/m^3 at T=22 °C and P$_0$=10^5 N/m^2),
S_D is the effective surface area of the diaphragm (m^2),
B is the magnetic flux density in the air gap (T),
l is the length of voice coil conductor in magnetic gap (m)

$$k_0 = \omega_1^2\,\omega_2^2\,\omega_3^2 \tag{5}$$

$$k_1 = \omega_1\,\omega_2\,\omega_3\left(\frac{\omega_1\,\omega_2}{Q_3} + \frac{\omega_1\,\omega_3}{Q_2} + \frac{\omega_2\,\omega_3}{Q_1}\right) \tag{6}$$

$$k_2 = \omega_1^2\,\omega_2^2 + \omega_1^2\,\omega_3^2 + \omega_2^2\,\omega_3^2 + \omega_1\,\omega_2\,\omega_3\left(\frac{\omega_1}{Q_2Q_3} + \frac{\omega_2}{Q_1Q_3} + \frac{\omega_3}{Q_1Q_2}\right) \tag{7}$$

$$k_3 = \frac{\omega_1(\omega_2^2+\omega_3^2)}{Q_1} + \frac{\omega_2(\omega_1^2+\omega_3^2)}{Q_2} + \frac{\omega_3(\omega_1^2+\omega_2^2)}{Q_3} + \frac{\omega_1\,\omega_2\,\omega_3}{Q_1\,Q_2\,Q_3} \tag{8}$$

$$k_4 = \omega_1^2 + \omega_2^2 + \omega_3^2 + \frac{\omega_1\,\omega_2}{Q_1\,Q_2} + \frac{\omega_1\,\omega_3}{Q_1\,Q_3} + \frac{\omega_2\,\omega_3}{Q_2\,Q_3} \tag{9}$$

$$k_5 = \frac{\omega_1}{Q_1} + \frac{\omega_2}{Q_2} + \frac{\omega_3}{Q_3} \tag{10}$$

The denominator polynomial in s can be tailored to produce a standard filter frequency-response shape. The resonant frequencies (ω_1, ω_2, ω_3) and their associated Q values are calculated from the real and imaginary parts of the root loci on the complex plane as follows

$$\omega_1 = \frac{1}{\sqrt{\alpha_1^2 + \beta_1^2}} \tag{11}$$

$$\omega_2 = \frac{1}{\sqrt{\alpha_2^2 + \beta_2^2}} \tag{12}$$

$$\omega_3 = \frac{1}{\sqrt{\alpha_3^2 + \beta_3^2}} \tag{13}$$

$$Q_1 = \frac{\sqrt{\alpha_1^2 + \beta_1^2}}{2\,\alpha_1} \tag{14}$$

$$Q_2 = \frac{\sqrt{\alpha_2^2 + \beta_2^2}}{2\,\alpha_2} \tag{14}$$

$$Q_3 = \frac{\sqrt{\alpha_3^2 + \beta_3^2}}{2\,\alpha_3} \tag{15}$$

where α_1, α_2 & α_3 are the real parts and β_1, β_2 & β_3 are the imaginary parts of the root loci. These are given for a selection of frequency response shapes in Table 1.

Frequency Response Shape	α_1	β_1	α_2	β_2	α_3	β_3	ω_1	Q_1	ω_2	Q_2	ω_3	Q_3
Synchronous	2.85759	0.00000	2.85759	0.00000	2.85759	0.00000	0.34995	0.50000	0.34995	0.50000	0.34995	0.50000
Bessel	1.57350	0.32130	1.38360	0.97270	0.93180	1.66400	0.62268	0.51032	0.59126	0.61120	0.52435	1.02336
$B3^2$ (Butterworth Squared)	1.00000	0.00000	0.50000	0.86603	0.50000	0.86603	1.00000	0.50000	1.00000	1.00000	1.00000	1.00000
B6 (Butterworth)	0.96593	0.25882	0.70711	0.70711	0.25882	0.96593	1.00000	0.51764	1.00000	0.70711	1.00000	1.93185
0.01dB Ripple Chebyshev	0.53353	0.25885	0.39057	0.70718	0.14296	0.96603	1.68633	0.55574	1.23783	1.03422	1.02401	3.41551
0.1dB Ripple Chebyshev	0.39165	0.25902	0.28670	0.70766	0.10494	0.96668	2.12969	0.59946	1.30970	1.33157	1.02842	4.63290
0.25dB Ripple Chebyshev	0.32840	0.25925	0.24040	0.70829	0.08799	0.96754	2.39007	0.63703	1.33695	1.55565	1.02930	5.52042
0.5dB Ripple Chebyshev	0.27837	0.25957	0.20378	0.70915	0.07459	0.96871	2.62734	0.68364	1.35529	1.81038	1.02925	6.51285

Table 1. Root Loci for a selection of 6th-Order Frequency Response Shapes

3 VENTED-BOX SYSTEM ALIGNMENTS WITH 2ND-ORDER ISOLATED FILTER (CLASSES I, II & III)

3.1 Transfer Function

A vented-box system with a 2nd-order isolated filter shown in Fig. 2. The actual transfer function that relates the sound pressure $p(r)$ at a distance r in free space for a given voltage e_{in} at the input of the filter is given by

$$p(r) = \frac{\left(\frac{A\,\rho_0\,S_D\,B\,l}{4\pi\,r\,M_{MD}\,(R_E+R_S)}\right)s^6\,e_{in}}{\left\{s^4+\left(\frac{\omega_S}{Q_{ES}}+\frac{\omega_B}{Q_L}\right)s^3+\left[\left(1+\frac{V_{AS}}{V_B}\right)\omega_S^2+\omega_B^2+\frac{\omega_S\,\omega_B}{Q_{ES}Q_L}\right]s^2+\omega_S\,\omega_B\left(\frac{\omega_S}{Q_L}+\frac{\omega_B}{Q_{ES}}\right)s+\omega_S^2\,\omega_B^2\right\}\left(s^2+\frac{\omega_E}{Q_{EI}}s+\omega_E^2\right)} \tag{16}$$

The normalised rms diaphragm displacement is given by

$$\frac{x}{x_{DC}} = \frac{\omega_S^2\left(s^2+\frac{\omega_B}{Q_L}s+\omega_B^2\right)s^2}{\left\{s^4+\left(\frac{\omega_S}{Q_{ES}}+\frac{\omega_B}{Q_L}\right)s^3+\left[\left(1+\frac{V_{AS}}{V_B}\right)\omega_S^2+\omega_B^2+\frac{\omega_S\,\omega_B}{Q_{ES}Q_L}\right]s^2+\omega_S\,\omega_B\left(\frac{\omega_S}{Q_L}+\frac{\omega_B}{Q_{ES}}\right)s+\omega_S^2\,\omega_B^2\right\}\left(s^2+\frac{\omega_E}{Q_{EI}}s+\omega_E^2\right)} \tag{17}$$

where x_{DC} is the displacement at DC of the driver in free space or a vented box, with no filter in either case, and is given by

$$x_{DC} = \frac{Bl\,C_{MS}}{R_E}\,e_{in} \tag{18}$$

The parameters C_{MS}, M_{MD} & Bl can be calculated from the Thiele-Small parameters R_E, f_S, Q_{ES}, V_{AS} & S_D as follows.

The mechanical suspension compliance C_{MS} is given by

$$C_{MS} = \frac{V_{AS}}{\rho_0\,c^2\,S_D^2} \tag{19}$$

where c is the speed of sound (=345 m/s at T=22 °C and $P_0=10^5$ N/m^2)

The mechanical moving mass (including the mass of the radiation load) is given by

$$M_{MD} = \frac{1}{(2\pi\,f_S)^2\,C_{MS}} \tag{20}$$

The magnetic flux and voice coil length product Bl is given by

$$Bl = \sqrt{\frac{R_E}{2\pi\,f_S\,C_{MS}\,Q_{ES}}} \tag{21}$$

Equating the polynomial coefficients of the two transfer functions, given by Eqs. (3) & (16), yields a set of six simultaneous equations. Solving these equations gives us the six following Eqs. (22) to (27) that are used to generate each alignment from the root loci

$$\frac{\omega_B^4}{Q_L}-\left(\frac{\omega_1}{Q_1}+\frac{\omega_2}{Q_2}\right)\omega_B^3+\omega_1\,\omega_2\left(\frac{\omega_1}{Q_2}+\frac{\omega_2}{Q_1}\right)\omega_B-\frac{\omega_1^2\,\omega_2^2}{Q_L}=0 \tag{22}$$

Eq. (22) above is solved for ω_B. Although this is a 4th-order polynomial with four roots, only one is positive and real.

$$\omega_S = \frac{\omega_1\,\omega_2}{\omega_B} \tag{23}$$

$$Q_{ES} = \frac{\omega_S}{\frac{\omega_1}{Q_1}+\frac{\omega_2}{Q_2}-\frac{\omega_B}{Q_L}} \tag{24}$$

$$\frac{V_{AS}}{V_B} = \frac{1}{\omega_S^2}\left(\omega_1^2+\omega_2^2+\frac{\omega_1\,\omega_2}{Q_1\,Q_2}-\omega_P^2-\frac{\omega_S\,\omega_B}{Q_{ES}\,Q_L}\right)-1 \tag{25}$$

$$\omega_E = \omega_3 \tag{26}$$

$$Q_{EI} = Q_3 \tag{27}$$

Eqs. (22) to (27) above provide the Class I alignments. To solve for Class II, swap ω_2 and ω_3 and also swap Q_2 and Q_3. To solve for Class III, swap ω_1 and ω_3 and also swap Q_1 and Q_3.

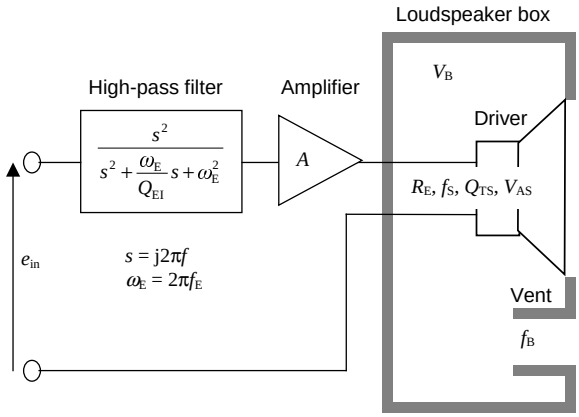

Fig. 2. Vented-box system with 2nd-order isolated filter

3.2 Class I Alignments

Response shape	$\frac{f_3}{f_S}$	$\frac{V_{AS}}{V_B}$	Q_{TS}	Q_{EI}	$\frac{f_E}{f_S}$	$\frac{f_B}{f_S}$
Synchronous	2.8576	3.4490	0.2593	0.5000	1.0000	1.0000
Bessel	1.6439	2.7016	0.2895	1.0234	0.8620	0.9950
$B3^2$	1.0000	1.5918	0.3500	1.0000	1.0000	1.0000
Butterworth	1.0000	2.2745	0.3122	1.9319	1.0000	1.0000
0.01dB Cheby	0.6574	1.3052	0.3770	3.4155	0.6732	0.9022
0.1dB Cheby	0.5404	0.9108	0.4283	4.6329	0.5558	0.8146
0.25dB Cheby	0.4882	0.7430	0.4667	5.5207	0.5025	0.7617
0.5dB Cheby	0.4477	0.6198	0.5118	6.5129	0.4608	0.7137

Table 2. Alignments for Class I lossy vented-box system with isolated 2nd-order high-pass filter

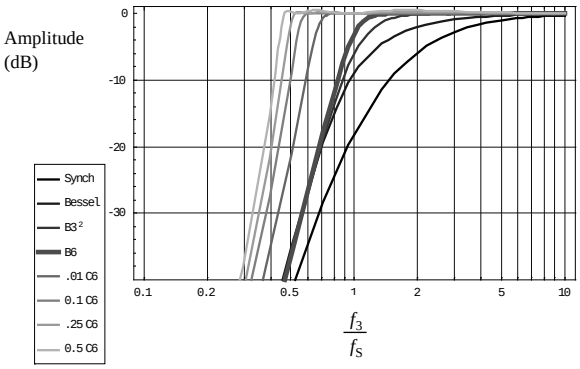

Fig. 3. Amplitude vs frequency plots for Class I lossy vented-box system with isolated 2nd-order high-pass filter

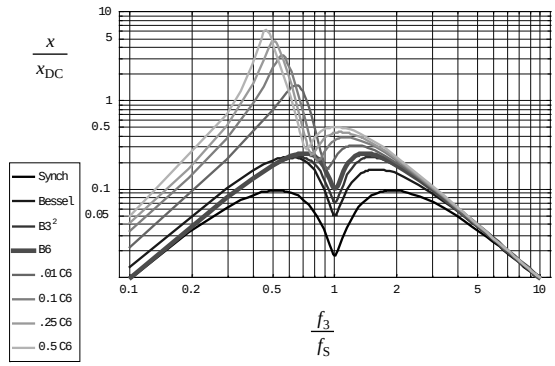

Fig. 4. Displacement vs frequency plots for Class I lossy vented-box system with isolated 2nd-order high-pass filter

3.3 Class II Alignments

Response shape	$\frac{f_3}{f_S}$	$\frac{V_{AS}}{V_B}$	Q_{TS}	Q_{EI}	$\frac{f_E}{f_S}$	$\frac{f_B}{f_S}$
Synchronous	2.8576	3.4490	0.2593	0.5000	1.0000	1.0000
Bessel	1.6954	1.4452	0.3567	0.6112	1.0024	0.9384
$B3^2$	1.0000	1.5918	0.3500	1.0000	1.0000	1.0000
Butterworth	1.0000	0.6705	0.4335	0.7071	1.0000	1.0000
0.01dB Cheby	0.6191	0.2162	0.5077	1.0342	0.7663	0.6618
0.1dB Cheby	0.4871	0.1130	0.5668	1.3316	0.6379	0.5196
0.25dB Cheby	0.4291	0.0654	0.6153	1.5556	0.5737	0.4530
0.5dB Cheby	0.3841	0.0207	0.6758	1.8104	0.5206	0.3989

Table 3. Alignments for Class II lossy vented-box system with isolated 2nd-order high-pass filter

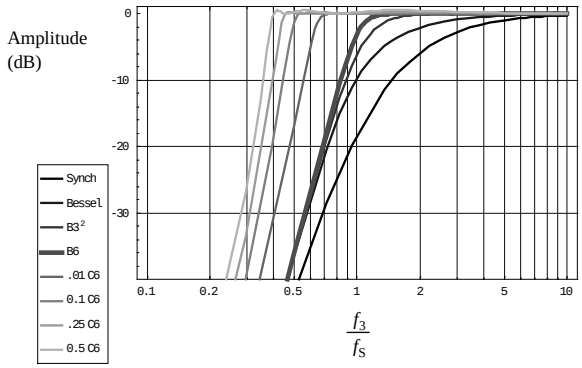

Fig. 5. Amplitude vs frequency plots for Class II lossy vented-box system with isolated 2nd-order high-pass filter

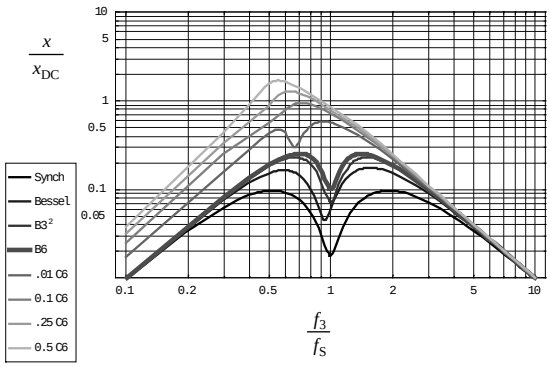

Fig. 6. Displacement vs frequency plots for Class II lossy vented-box system with isolated 2nd-order high-pass filter

3.4 Class III Alignments

Response shape	$\frac{f_3}{f_S}$	$\frac{V_{AS}}{V_B}$	Q_{TS}	Q_{EI}	$\frac{f_E}{f_S}$	$\frac{f_B}{f_S}$
Synchronous	2.8576	3.4490	0.2593	0.5000	1.0000	1.0000
Bessel	1.7657	1.2165	0.4041	0.5103	1.0995	0.9666
$B3^2$	1.0000	0.7347	0.5385	0.5000	1.0000	1.0000
Butterworth	1.0000	0.4765	0.5590	0.5176	1.0000	1.0000
0.01dB Cheby	0.8319	0.1246	0.8930	0.5557	1.4029	0.8773
0.1dB Cheby	0.7838	0.0553	1.2096	0.5995	1.6692	0.8275
0.25dB Cheby	0.7623	0.0299	1.4642	0.6370	1.8218	0.7996
0.5dB Cheby	0.7432	0.0093	1.7739	0.6837	1.9525	0.7704

Table 4. Alignments for Class III lossy vented-box system with isolated 2nd-order high-pass filter

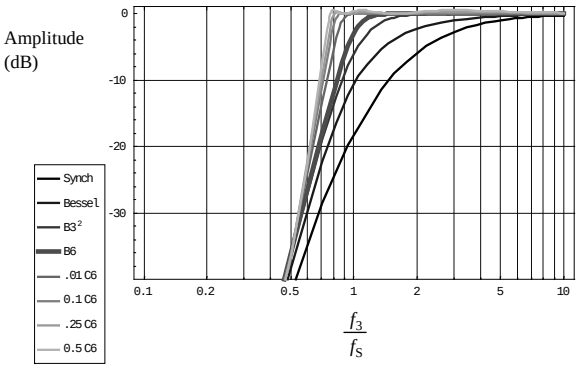

Fig. 7. Amplitude vs frequency plots for Class III lossy vented-box system with isolated 2nd-order high-pass filter

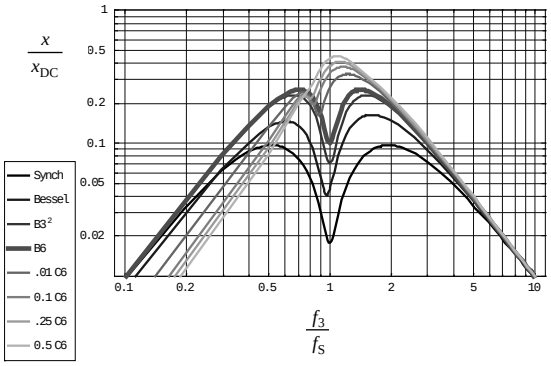

Fig. 8. Displacement vs frequency plots for Class III lossy vented-box system with isolated 2nd-order high-pass filter

4 VENTED-BOX SYSTEM ALIGNMENTS WITH 2ND-ORDER NON-ISOLATED FILTER (TYPES 1, 2 & 3)

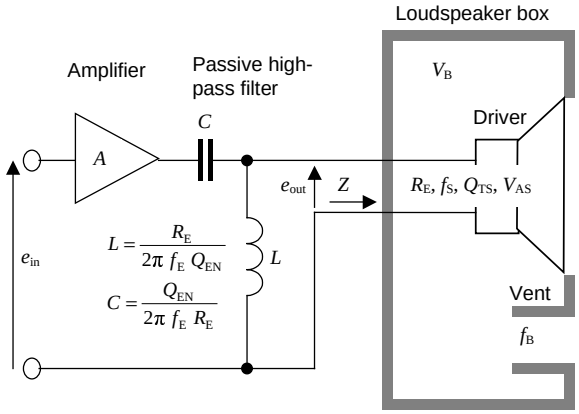

Fig. 9. Vented-box system with passive 2nd-order non-isolated filter

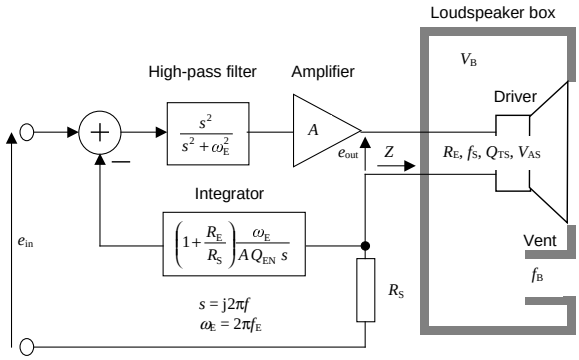

Fig. 10. Vented-box system with active 2nd-order non-isolated filter

4.1 Transfer Function

A vented-box system with a 2nd-order non-isolated filter shown in Figs. 9 and 10. The actual transfer function that relates the sound pressure $p(r)$ at a distance r in free space for a given voltage e_{in} at the input of the filter is given by

$$p(r) = \frac{\left(\frac{A\,\rho_0\,S_D\,B\,l}{4\pi\,r\,M_{MD}\,(R_E + R_S)}\right) s^6\,e_{in}}{\left\{ s^6 + \left(\frac{\omega_S}{Q_{ES}} + \frac{\omega_B}{Q_L} + \frac{\omega_E}{Q_{EN}}\right)s^5 + \left[\left(1+\frac{V_{AS}}{V_B}\right)\omega_S^2 + \omega_B^2 + \omega_E^2 + \frac{\omega_S\,\omega_B}{Q_{ES}\,Q_L} + \frac{\omega_B\,\omega_E}{Q_L\,Q_{EN}}\right]s^4 + \left[\omega_S^2\left(\frac{\omega_B}{Q_L} + \left(1+\frac{V_{AS}}{V_B}\right)\frac{\omega_E}{Q_{EN}}\right) + \omega_B^2\left(\frac{\omega_S}{Q_{ES}} + \frac{\omega_E}{Q_{EN}}\right) + \omega_E^2\left(\frac{\omega_S}{Q_{ES}} + \frac{\omega_B}{Q_L}\right)\right]s^3 \right.$$
$$\left. + \left[\omega_S^2\,\omega_B^2 + \left(1+\frac{V_{AS}}{V_B}\right)\omega_S^2\,\omega_E^2 + \omega_B^2\,\omega_E^2 + \omega_S\,\omega_B\,\omega_E\left(\frac{\omega_S}{Q_L\,Q_{EN}} + \frac{\omega_E}{Q_{ES}\,Q_L}\right)\right]s^2 + \omega_S\,\omega_B\,\omega_E\left(\frac{\omega_S\,\omega_B}{Q_{EN}} + \frac{\omega_S\,\omega_E}{Q_L} + \frac{\omega_B\,\omega_E}{Q_{ES}}\right)s + \omega_S^2\,\omega_B^2\,\omega_E^2 \right\} \quad (28)$$

The normalised rms diaphragm displacement is given by

$$\frac{x}{x_{DC}} = \frac{\omega_S^2\left(s^2 + \frac{\omega_B}{Q_L}s + \omega_B^2\right)s^2}{\left\{ s^6 + \left(\frac{\omega_S}{Q_{ES}} + \frac{\omega_B}{Q_L} + \frac{\omega_E}{Q_{EN}}\right)s^5 + \left[\left(1+\frac{V_{AS}}{V_B}\right)\omega_S^2 + \omega_B^2 + \omega_E^2 + \frac{\omega_S\,\omega_B}{Q_{ES}\,Q_L} + \frac{\omega_B\,\omega_E}{Q_L\,Q_{EN}}\right]s^4 + \left[\omega_S^2\left(\frac{\omega_B}{Q_L} + \left(1+\frac{V_{AS}}{V_B}\right)\frac{\omega_E}{Q_{EN}}\right) + \omega_B^2\left(\frac{\omega_S}{Q_{ES}} + \frac{\omega_E}{Q_{EN}}\right) + \omega_E^2\left(\frac{\omega_S}{Q_{ES}} + \frac{\omega_B}{Q_L}\right)\right]s^3 \right.$$
$$\left. + \left[\omega_S^2\,\omega_B^2 + \left(1+\frac{V_{AS}}{V_B}\right)\omega_S^2\,\omega_E^2 + \omega_B^2\,\omega_E^2 + \omega_S\,\omega_B\,\omega_E\left(\frac{\omega_S}{Q_L\,Q_{EN}} + \frac{\omega_E}{Q_{ES}\,Q_L}\right)\right]s^2 + \omega_S\,\omega_B\,\omega_E\left(\frac{\omega_S\,\omega_B}{Q_{EN}} + \frac{\omega_S\,\omega_E}{Q_L} + \frac{\omega_B\,\omega_E}{Q_{ES}}\right)s + \omega_S^2\,\omega_B^2\,\omega_E^2 \right\} \quad (29)$$

Equating the polynomial coefficients of the two transfer functions, given by Eqs. (4) & (28), yields a set of six simultaneous equations. Solving these equations gives us the six following Eqs. (30) to (35) that are used to generate each alignment from the root loci

$$Q_L^2\,\omega_B^2\,\omega_E^6 - \left(\omega_B^4 - k_5\,Q_L\,\omega_B^3 + k_4\,Q_L^2\,\omega_B^2\right)\omega_E^4 + \left(k_2\,Q_L^2\,\omega_B^2 - k_1\,Q_L\,\omega_B + k_0\right)\omega_E^2 - k_0\,Q_L^2\,\omega_B^2 = 0 \quad (30)$$

$$\left(2Q_L^2\,\omega_B^4 - k_5\,Q_L^3\,\omega_B^3\right)\omega_E^8 - \left[\omega_B^6 - 2k_5\,Q_L\,\omega_B^5 + \left(k_4 + k_5^2\right)Q_L^2\,\omega_B^4 + \left(k_3 - k_4\,k_5\right)Q_L^3\,\omega_B^3 - 2k_1\,Q_L^3\,\omega_B + 2k_0\,Q_L^2\right]\omega_E^6$$
$$+ \left[k_1\left(Q_L^2 - 1\right)Q_L\,\omega_B^3 + \left(k_0 + k_1\,k_5\,Q_L^2\right)\omega_B^2 - \left(k_0\,k_5\left(Q_L^2 + 1\right) + k_1\,k_4\,Q_L^2\right)Q_L\,\omega_B + k_0\,k_4\,Q_L^2\right]\omega_E^4 + k_0\,Q_L^2\left(\omega_B^4 - k_5\,Q_L\,\omega_B^3 + k_5\,Q_L\,\omega_B\right)\omega_E^2 - k_0^2\,Q_L^2 = 0 \quad (31)$$

Eqs. (30) & (31) above are solved simultaneously for ω_B & ω_E. Although these are a high-order polynomials with many roots, only a maximum of three are positive and real and these give rise to the Type 1, 2 & 3 solutions.

$$\left[\frac{\omega_B^4}{Q_L} - k_5\,\omega_B^3 - \left(k_5\,\omega_E^2 - k_3\right)\omega_B - \frac{\omega_E^4 - k_4\,\omega_E^2 + k_2}{Q_L}\right]Q_{EN}^2 + \left[\omega_B^3 + \left\{\left(2 - \frac{1}{Q_L^2}\right)\omega_E^2 - k_4\right\}\omega_B - \frac{k_5\,\omega_E^2 - k_3}{Q_L}\right]Q_{EN} + \frac{\omega_E^2}{Q_L}\left[\left(1 - \frac{1}{Q_L^2}\right)\omega_B^2 + \frac{k_5}{Q_L}\omega_B + 2\,\omega_E^2 - k_4\right] = 0 \quad (32a)$$

In the case of Type 1 or Type 2, the above equation (32a) is solved for Q_{EN}. The positive real solution is selected. In the case of Type 3, the following alternative equation (32b) applies

$$Q_{EN} = \frac{\omega_B\left(\omega_E^4\,\omega_B^2 - k_0\right)}{\omega_E\left[\omega_E^2\,\omega_B^3\left(k_5 - \frac{\omega_B}{Q_L}\right) - k_1\,\omega_B + \frac{k_0}{Q_L}\right]} \quad (32b)$$

$$\frac{V_{AS}}{V_B} = -\frac{\omega_E^4 + \frac{2\omega_B\,\omega_E^3}{Q_L\,Q_{EN}} + \left(\omega_B^2 - k_4\right)\omega_E^2 + \left[\left(1 - \frac{1}{Q_L^2}\right)\omega_B^2 + \frac{k_5\,\omega_B}{Q_L} - k_4\right]\left(\frac{\omega_B\,\omega_E}{Q_L\,Q_{EN}} + \omega_B^2\right) + k_2}{k_0\left(\omega_B + \frac{\omega_E}{Q_L\,Q_{EN}}\right)}\,\omega_B\,\omega_E^2 \quad (33)$$

$$\omega_S = \frac{\sqrt{k_0}}{\omega_B\,\omega_E} \quad (34)$$

$$Q_{ES} = \frac{\omega_S}{k_5 - \frac{\omega_B}{Q_L} - \frac{\omega_E}{Q_{EN}}} \quad (35)$$

4.2 Type 1 Alignments

Response shape	$\frac{f_3}{f_S}$	$\frac{V_{AS}}{V_B}$	Q_{TS}	Q_{EN}	$\frac{f_E}{f_S}$	$\frac{f_B}{f_S}$
Synchronous	1.2254	1.0512	0.4311	0.7463	0.1169	0.6744
Bessel	0.8059	0.5637	0.5306	0.8077	0.1643	0.6149
$B3^2$	0.4969	0.3736	0.6016	0.8298	0.1956	0.6270
Butterworth	0.4890	0.2585	0.6416	0.8134	0.2017	0.5799
0.01dB Cheby	0.4088	0.2354	0.6602	1.0538	0.2762	0.5287
0.1dB Cheby	0.3954	0.2978	0.6318	1.4646	0.3221	0.5505
0.25dB Cheby	0.3905	0.3375	0.6188	1.9485	0.3426	0.5716
0.5dB Cheby	0.3833	0.3581	0.6229	2.6829	0.3534	0.5841

Table 5. Alignments for Type 1 lossy vented-box system with non-isolated 2nd-order high-pass filter

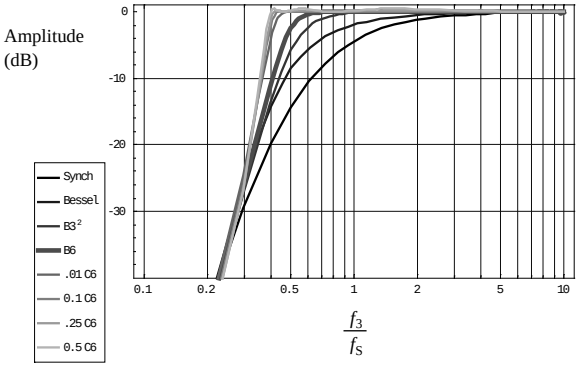

Fig. 11. Amplitude vs frequency plots for Type 1 vented-box system with non-isolated 2nd-order high-pass filter

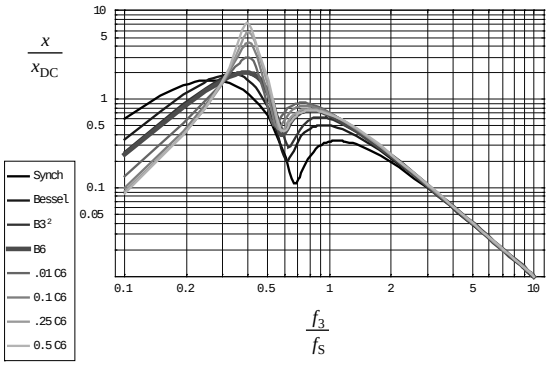

Fig. 12. Displacement vs frequency plots for Type 2 lossy vented-box system with non-isolated 2nd-order high-pass filter

4.3 Type 2 Alignments

Response shape	$\frac{f_3}{f_S}$	$\frac{V_{AS}}{V_B}$	Q_{TS}	Q_{EN}	$\frac{f_E}{f_S}$	$\frac{f_B}{f_S}$
Synchronous	2.8576	11.163	0.1945	1.3954	1.0000	1.0000
Bessel	1.6865	5.9593	0.2552	1.9214	0.9530	0.9717
$B3^2$	1.0000	4.4489	0.2935	2.2245	1.0000	1.0000
Butterworth	1.0000	3.9326	0.2975	2.7807	1.0000	1.0000
0.01dB Cheby	0.6603	1.9247	0.3784	3.2249	0.7445	0.8264
0.1dB Cheby	0.5263	1.1962	0.4567	2.8248	0.6136	0.6817
0.25dB Cheby	0.4567	0.8342	0.5280	2.5184	0.5396	0.5808
0.5dB Cheby	0.3909	0.4893	0.6325	2.2314	0.4647	0.4710

Table 6. Alignments for Type 2 lossy vented-box system with non-isolated 2nd-order high-pass filter

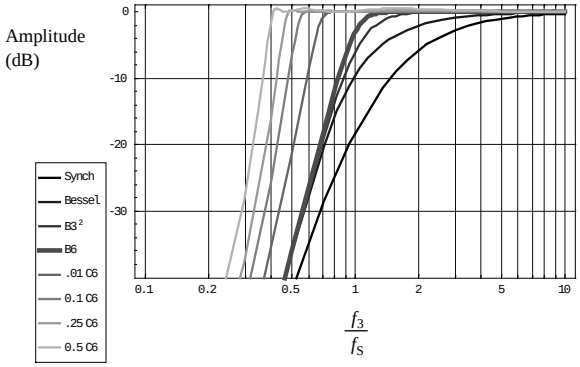

Fig. 13. Amplitude vs frequency plots for Type 2 lossy vented-box system with non-isolated 2nd-order high-pass filter

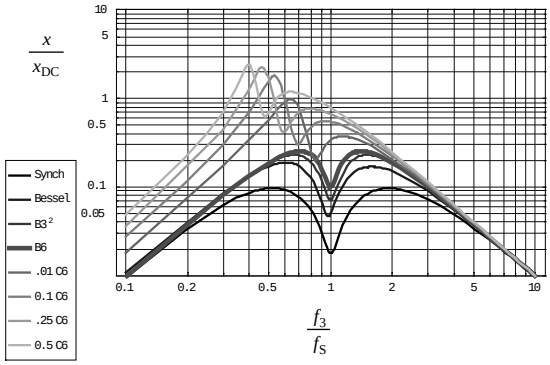

Fig. 14. Displacement vs frequency plots for Type 2 lossy vented-box system with non-isolated 2nd-order high-pass filter

4.4 Type 3 Alignments

Response shape	$\frac{f_3}{f_S}$	$\frac{V_{AS}}{V_B}$	Q_{TS}	Q_{EN}	$\frac{f_E}{f_S}$	$\frac{f_B}{f_S}$
Synchronous	6.6640	2.3115	0.4311	0.7463	8.5526	1.4829
Bessel	3.6820	1.2276	0.5515	0.7897	6.1716	1.5615
$B3^2$	2.0126	0.9503	0.6016	0.8298	5.1115	1.5948
Butterworth	2.0448	0.7688	0.6416	0.8134	4.9580	1.7246
0.01dB Cheby	1.3431	0.1394	0.8641	0.8041	3.8065	1.3605
0.1dB Cheby	1.0969	0.0515	1.0766	0.8048	3.3220	1.1395
0.25dB Cheby	0.9917	0.0260	1.2643	0.8139	3.1086	1.0318
0.5dB Cheby	0.9118	0.0077	1.5092	0.8338	2.9461	0.9430

Table 7. Alignments for Type 3 lossy vented-box system with non-isolated 2nd-order high-pass filter

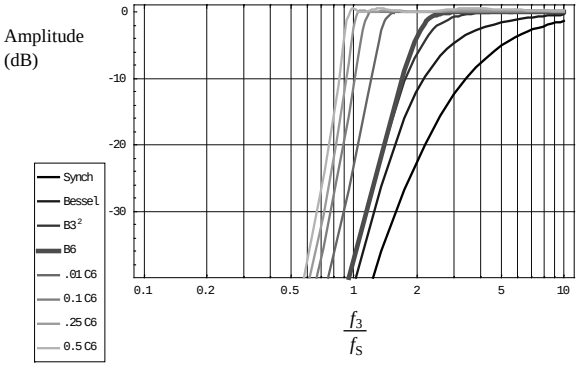

Fig. 15. Amplitude vs frequency plots for Type 3 lossy vented-box system with non-isolated 2nd-order high-pass filter

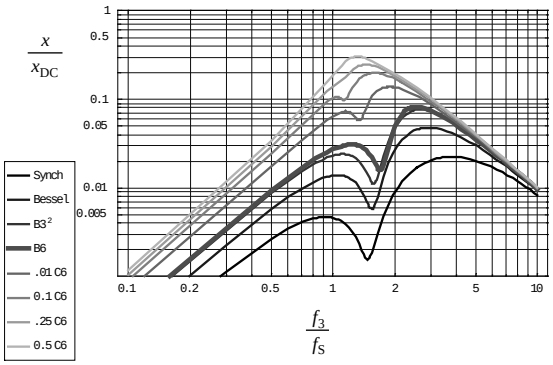

Fig. 16. Displacement vs frequency plots for Type 3 lossy vented-box system with non-isolated 2nd-order high-pass filter

5 2ND-ORDER LEMF

The LEMF scheme shown in Fig. 17 has already been discussed in some detail in Part 1 in which a set of loss-less B6 Butterworth alignments was presented. Here, some LEMF alignments for alternative frequency response shapes will be presented together with correction factors for lossy vented boxes with a Q_L value of 7. By examining the 6th-order isolated and non-isolated alignments given in sections 4 and 5, it looks as though we can disregard Chebyshev alignments with a ripple of greater than 0.01 dB because they result in excessive diaphragm displacement in the cases of Class I, Class II, Type 1 and Type 2 alignments. Also, the box volume requirement becomes impractical in the cases of Class III and Type 3 alignments. Another problem, in the case of Class I, is that of power lift, which is approximately equal to Q_{EI}^2 (if we ignore the fact that the impedance is not equal to R_E at all frequencies). This presents several potential problems as follows

- The amplifier can run into premature clipping if it is not powerful enough.
- The driver can burn out if it is not of a high enough power rating.
- Power compression can occur. This is a phenomenon whereby the heating of the voice coil causes R_E to drop temporarily, which then leads to a short-term reduction in the acoustic output.

However, if these problems can be addressed, power lift is an effective way of utilising a smaller box. An added bonus is that the resulting high compliance ratio reduces distortion due to suspension non-linearity at frequencies above the box resonance. It also increases immunity to variation in C_{MS}, which, in practice, is one of the most unreliable parameters.

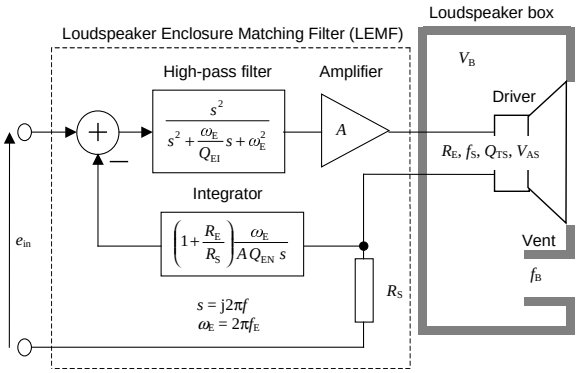

Fig. 17: Vented-box system with 2nd-order LEMF

Because of the problems mentioned above, only the 0.01 dB Chebyshev LEMF alignments are presented here as shown in Table 8. There seems little point in deriving a plethora of sub-Butterworth alignments either, as their useful working range is somewhat limited. Instead, just two have been chosen because they could be useful in certain applications. There has been much debate over the poor time domain response of Butterworth alignments and the tendency for step inputs to produce undershoot and subsequent ringing at the tail of the response. Therefore, designers, for whom this may be a cause of concern, may wish to consider the use of the Bessel alignments shown in Table 9, as these exhibit fairly optimal time domain behavior [2]. A frequency response shape that usefully fills the gap between Bessel and Butterworth is the 3rd-order Butterworth squared ($B3^2$) shape, which forms a constant-resistance loudspeaker crossover function, and alignments for this are given in Table 10. Unlike all the other alignments, where f_3 denotes the -3dB point (relative to the pass-band level), in the case of the $B3^2$ alignments f_3 is the crossover frequency. As such, it actually represents the -6 dB point. This function could be used, for example, to integrate vented-box satellites with a sub-woofer.

Q_{EI}	Type 1 0.01dB Chebyshev LEMF alignments						Type 2 0.01dB Chebyshev LEMF alignments						Type 3 0.01dB Chebyshev LEMF alignments					
	f_3/f_S	V_{AS}/V_B	Q_{TS}	Q_{EN}	f_E/f_S	f_B/f_S	f_3/f_S	V_{AS}/V_B	Q_{TS}	Q_{EN}	f_E/f_S	f_B/f_S	f_3/f_S	V_{AS}/V_B	Q_{TS}	Q_{EN}	f_E/f_S	f_B/f_S
Inf.	Type 1 0.01C6 Alignment with Non-Isolated Filter						Type 2 0.01C6 Alignment with Non-Isolated Filter						Type 3 0.01C6 Alignment with Non-Isolated Filter					
	0.408	0.340	0.626	1.050	0.262	0.553	0.670	2.345	0.352	3.820	0.760	0.848	1.374	0.316	0.801	0.811	4.036	1.374
10.00	0.416	0.351	0.617	1.159	0.274	0.561	0.668	2.109	0.356	5.325	0.746	0.853	1.352	0.316	0.794	0.872	3.904	1.354
8.000	0.418	0.354	0.615	1.190	0.277	0.563	0.667	2.051	0.357	5.895	0.741	0.855	1.347	0.316	0.793	0.888	3.870	1.349
7.000	0.420	0.356	0.613	1.213	0.280	0.564	0.666	2.009	0.357	6.383	0.738	0.857	1.343	0.316	0.791	0.901	3.846	1.345
5.000	0.425	0.363	0.608	1.293	0.288	0.569	0.664	1.878	0.360	8.745	0.724	0.864	1.330	0.315	0.787	0.942	3.769	1.333
4.000	0.430	0.369	0.603	1.372	0.296	0.574	0.662	1.763	0.361	13.83	0.707	0.876	1.318	0.315	0.784	0.981	3.701	1.323
3.416	0.435	0.375	0.599	1.447	0.304	0.578	Class I 0.01C6 Alignment with Isolated Filter						1.308	0.315	0.781	1.017	3.642	1.314
							0.661	1.666	0.358	Inf.	0.677	0.912						
3.000	0.439	0.380	0.595	1.526	0.311	0.582							1.298	0.315	0.778	1.054	3.585	1.305
2.500	0.447	0.390	0.588	1.675	0.324	0.588							1.282	0.315	0.773	1.119	3.490	1.290
2.000	0.460	0.405	0.577	1.960	0.348	0.599							1.256	0.314	0.765	1.233	3.345	1.267
1.500	0.487	0.430	0.558	2.718	0.400	0.618							1.211	0.313	0.753	1.478	3.095	1.226
1.200	0.524	0.449	0.537	4.358	0.482	0.640							1.161	0.312	0.740	1.828	2.833	1.181
1.034	0.575	0.448	0.513	9.348	0.611	0.667	Class II 0.01C6 Alignment with Isolated Filter						1.118	0.311	0.731	2.233	2.613	1.142
							0.637	0.458	0.471	Inf.	0.789	0.701						
1.010	0.600	0.447	0.499	15.56	0.678	0.680	0.615	0.449	0.489	25.42	0.721	0.689	1.110	0.311	0.730	2.319	2.574	1.135
0.900													1.067	0.309	0.723	2.884	2.367	1.097
0.800													1.015	0.306	0.717	3.885	2.126	1.051
0.700													0.946	0.300	0.721	6.318	1.826	0.990
0.600													0.871	0.288	0.756	18.56	1.525	0.926
0.556													Class III 0.01C6 Alignment with Isolated Filter					
													0.844	0.279	0.791	Inf.	1.424	0.904

Table 8. 0.01dB Chebyshev (C6) alignments for loss-less vented-box system with 2nd-order LEMF

Q_{EI}	Type 1 Bessel LEMF alignments						Type 2 Bessel LEMF alignments						Type3 Bessel LEMF alignments					
	f_3/f_S	V_{AS}/V_B	Q_{TS}	Q_{EN}	f_E/f_S	f_B/f_S	f_3/f_S	V_{AS}/V_B	Q_{TS}	Q_{EN}	f_E/f_S	f_B/f_S	f_3/f_S	V_{AS}/V_B	Q_{TS}	Q_{EN}	f_E/f_S	f_B/f_S
Inf.	Type 1 Bessel Alignment Non-Isolated Filter						Type 2 Bessel Alignment Non-Isolated Filter						Type 3 Bessel Alignment with Non-Isolated Filter					
	0.801	0.712	0.509	0.812	0.159	0.623	1.689	6.594	0.243	2.120	0.955	0.974	3.709	1.553	0.527	0.785	6.376	1.545
10.00	0.813	0.730	0.503	0.873	0.164	0.631	1.688	6.198	0.245	2.488	0.953	0.975	3.658	1.557	0.521	0.843	6.186	1.528
8.000	0.816	0.735	0.501	0.890	0.166	0.632	1.688	6.100	0.246	2.597	0.953	0.975	3.645	1.558	0.520	0.858	6.138	1.524
7.000	0.818	0.739	0.500	0.902	0.167	0.634	1.688	6.030	0.246	2.680	0.952	0.975	3.636	1.559	0.519	0.870	6.104	1.520
5.000	0.825	0.751	0.497	0.944	0.170	0.638	1.687	5.804	0.247	2.978	0.951	0.975	3.606	1.561	0.515	0.908	5.993	1.510
4.000	0.831	0.761	0.494	0.983	0.173	0.642	1.686	5.613	0.248	3.288	0.950	0.975	3.579	1.564	0.512	0.945	5.894	1.501
3.000	0.843	0.780	0.488	1.057	0.178	0.649	1.685	5.300	0.250	3.939	0.947	0.976	3.532	1.568	0.507	1.013	5.727	1.485
2.500	0.853	0.796	0.484	1.123	0.183	0.655	1.684	5.054	0.252	4.630	0.945	0.976	3.494	1.571	0.503	1.073	5.591	1.472
2.000	0.868	0.822	0.477	1.239	0.190	0.664	1.674	4.643	0.257	6.057	0.935	0.972	3.434	1.576	0.496	1.179	5.382	1.452
1.500	0.896	0.867	0.466	1.474	0.204	0.679	1.677	4.124	0.261	11.15	0.930	0.979	3.328	1.586	0.485	1.404	5.020	1.417
1.023	0.964	0.980	0.442	2.267	0.241	0.716	Class I Bessel Alignment with Isolated Filter						3.102	1.610	0.461	2.126	4.286	1.344
							1.644	3.194	0.278	Inf.	0.862	0.995						
0.900	1.002	1.041	0.431	2.882	0.263	0.734							2.988	1.623	0.449	2.687	3.939	1.308
0.800	1.049	1.115	0.418	3.890	0.292	0.756							2.856	1.639	0.436	3.624	3.551	1.267
0.700	1.152	1.286	0.395	7.653	0.369	0.799							2.657	1.664	0.417	6.107	2.999	1.207
0.611	1.328	1.501	0.370	25.49	0.527	0.856	Class II Bessel Alignment with Isolated Filter						2.348	1.697	0.392	16.95	2.234	1.119
							1.701	1.833	0.339	Inf.	1.006	0.944						
0.600	1.365	1.534	0.367	33.16	0.566	0.866	1.751	1.832	0.340	2179	1.072	0.961	2.291	1.701	0.388	21.27	2.105	1.104
0.570	1.499	1.612	0.360	84.94	0.720	0.900	1.744	1.742	0.351	266.1	1.059	0.962	2.097	1.704	0.376	51.25	1.693	1.052
0.550	1.625	1.642	0.360	169.1	0.883	0.933	1.720	1.677	0.359	216.7	1.021	0.957	1.924	1.682	0.370	127.8	1.364	1.008
0.530	1.729	1.623	0.368	254.3	1.033	0.961	1.711	1.620	0.368	242.2	1.005	0.956	1.810	1.623	0.374	283.1	1.169	0.979
0.520	1.730	1.595	0.373	351.3	1.034	0.962	1.719	1.594	0.373	327.2	1.016	0.959	1.789	1.592	0.378	541.6	1.136	0.974
0.510							Class III Bessel Alignment with Isolated Filter											
							1.769	1.564	0.382	Inf.	1.102	0.970						

Table 9. Bessel (Be6) alignments for loss-less vented-box system with 2nd-order LEMF

Q_{EI}	Type 1 $B3^2$ LEMF alignments						Type 2 $B3^2$ LEMF alignments						Type 3 $B3^2$ LEMF alignments					
	f_3/f_S	V_{AS}/V_B	Q_{TS}	Q_{EN}	f_E/f_S	f_B/f_S	f_3/f_S	V_{AS}/V_B	Q_{TS}	Q_{EN}	f_E/f_S	f_B/f_S	f_3/f_S	V_{AS}/V_B	Q_{TS}	Q_{EN}	f_E/f_S	f_B/f_S
Inf.	Type 1 $B3^2$ Alignment with Non-Isolated Filter						Type 2 $B3^2$ Alignment with Non-Isolated Filter						Type 3 $B3^2$ Alignment with Non-Isolated Filter					
	0.492	0.501	0.574	0.833	0.188	0.635	1.000	5.000	0.278	2.500	1.000	1.000	2.031	1.244	0.574	0.833	5.318	1.576
10.00	0.500	0.515	0.567	0.898	0.195	0.643	1.000	4.643	0.280	3.023	1.000	1.000	2.000	1.247	0.567	0.898	5.141	1.556
8.000	0.502	0.519	0.565	0.916	0.196	0.645	1.000	4.555	0.281	3.184	1.000	1.000	1.992	1.248	0.565	0.916	5.096	1.551
7.000	0.503	0.521	0.564	0.929	0.198	0.646	1.000	4.492	0.281	3.307	1.000	1.000	1.986	1.249	0.564	0.929	5.063	1.548
5.000	0.508	0.530	0.560	0.974	0.202	0.651	1.000	4.293	0.283	3.761	1.000	1.000	1.968	1.251	0.560	0.974	4.959	1.536
4.000	0.513	0.538	0.557	1.016	0.206	0.656	1.000	4.121	0.285	4.250	1.000	1.000	1.951	1.252	0.557	1.016	4.866	1.526
3.000	0.520	0.552	0.550	1.095	0.212	0.663	1.000	3.840	0.287	5.334	1.000	1.000	1.922	1.255	0.550	1.095	4.708	1.508
2.500	0.527	0.564	0.546	1.166	0.218	0.670	1.000	3.621	0.290	6.564	1.000	1.000	1.898	1.258	0.546	1.166	4.579	1.493
2.000	0.538	0.584	0.538	1.292	0.228	0.680	1.000	3.303	0.295	9.474	1.000	1.000	1.860	1.262	0.538	1.292	4.381	1.470
1.500	0.558	0.622	0.524	1.567	0.248	0.700	1.000	2.808	0.304	21.96	1.000	1.000	1.793	1.270	0.524	1.567	4.034	1.428
1.000	0.613	0.726	0.493	2.631	0.307	0.751	Class I & II $B3^2$ Alignment with Isolated Filter						1.631	1.289	0.493	2.631	3.258	1.332
							1.000	2.000	0.333	Inf.	1.000	1.000						
0.900	0.639	0.774	0.481	3.333	0.337	0.773	1.000	1.794	0.347	276.0	1.000	1.000	1.565	1.297	0.481	3.333	2.964	1.294
0.800	0.681	0.851	0.464	4.852	0.391	0.806	1.000	1.581	0.366	67.06	1.000	1.000	1.469	1.308	0.464	4.852	2.557	1.240
0.700	0.768	0.997	0.440	10.01	0.521	0.869	1.000	1.370	0.394	32.50	1.000	1.000	1.302	1.320	0.440	10.01	1.920	1.151
0.680	0.801	1.047	0.433	12.78	0.577	0.891	1.000	1.330	0.401	29.79	1.000	1.000	1.248	1.320	0.433	12.78	1.732	1.123
0.660	0.851	1.113	0.425	17.46	0.669	0.921	1.000	1.289	0.408	27.86	1.000	1.000	1.175	1.313	0.425	17.46	1.494	1.086
0.650	0.891	1.158	0.421	21.20	0.749	0.943	1.000	1.270	0.412	27.18	1.000	1.000	1.123	1.303	0.421	21.20	1.335	1.060
0.600							1.000	1.174	0.436	26.67	1.000	1.000						
0.550							1.000	1.083	0.464	36.06	1.000	1.000						
0.500							Class III $B3^2$ Alignment with Isolated Filter											
							1.000	1.000	0.500	Inf.	1.000	1.000						

Table 10. 3rd-order Butterworth squared ($B3^2$) alignments for loss-less vented-box system with 2nd-order LEMF

Correction factors for the isolated and non-isolated filter assisted alignments at the extremes of the LEMF range are shown in Tables 11 and 12 respectively. The most significant correction factors appear to be those for V_B. It should be possible to extrapolate values for the LEMF alignments that fall between these extremes. A global factor of 1.06 could be applied for Q_{TS} with reasonable accuracy. The remaining parameters appear to require little or no correction except for Q_{EN} in the case of Type 2 non-isolated alignments. Again, as in the case of V_B, some extrapolation is required to estimate suitable values for LEMF in-between alignments. If the Q_L value is greater than 7, then smaller correction factors can be estimated.

Response	Class I					Class II					Class III				
Shape	V_B	Q_{TS}	Q_{EN}	f_E	f_B	V_B	Q_{TS}	Q_{EN}	f_E	f_B	V_B	Q_{TS}	Q_{EN}	f_E	f_B
Bessel	1.18	1.04	1	1	1	1.27	1.05	1	1	0.99	1.29	1.06	1	1	1
$B3^2$	1.26	1.05	1	1	1	1.26	1.05	1	1	1	1.36	1.08	1	1	1
B6	1.20	1.04	1	1	1	1.49	1.06	1	1	1	1.54	1.08	1	1	1
0.01dB C6	1.28	1.05	1	0.99	0.99	2.12	1.08	1	0.97	0.94	2.24	1.13	1	0.99	0.97

Table 11. Correction factors for lossy vented-box system alignments with isolated 2nd-order filter and a Q_L value of 7

Response	Type 1					Type 2					Type 3				
Shape	V_B	Q_{TS}	Q_{EN}	f_E	f_B	V_B	Q_{TS}	Q_{EN}	f_E	f_B	V_B	Q_{TS}	Q_{EN}	f_E	f_B
Bessel	1.26	1.04	1	1.03	0.99	1.11	1.05	0.91	1	1	1.27	1.05	1.01	0.97	1.01
$B3^2$	1.34	1.05	1	1.04	0.99	1.12	1.06	0.89	1	1	1.31	1.05	1	0.96	1.01
B6	1.47	1.06	0.99	1.04	0.97	1.14	1.06	0.88	1	1	1.39	1.06	0.99	0.96	1.03
0.01dB C6	1.44	1.06	1	1.05	0.96	1.22	1.08	0.84	0.98	0.98	2.27	1.08	0.99	0.94	0.99

Table 12. Correction factors for lossy vented-box system alignments with non-isolated 2nd-order filter and a Q_L value of 7

6 5TH-ORDER FREQUENCY RESPONSE SHAPES

A generic 5th-order high-pass system transfer-function that relates the sound pressure $p(r)$ at a distance r in free space for a given voltage e_{in} at the input of the LEMF is given by

$$p(r) = \frac{\left(\frac{A\rho_0 S_D B l}{4\pi r M_{MD}(R_E + R_S)}\right) s^5 e_{in}}{\left(s^2 + \frac{\omega_1}{Q_1}s + \omega_1^2\right)\left(s^2 + \frac{\omega_2}{Q_2}s + \omega_2^2\right)(s + \omega_3)} \quad (36)$$

$$= \frac{\left(\frac{A\rho_0 S_D B l}{4\pi r M_{MD}(R_E + R_S)}\right) s^5 e_{in}}{s^5 + k_4 s^4 + k_3 s^3 + k_2 s^2 + k_1 s + k_0} \quad (37)$$

where

ρ_0 is the density of air (=1.18 kg/m^3 at T=22 °C and P$_0$=10^5 N/m^2),
S_D is the effective surface area of the diaphragm (m^2),
B is the magnetic flux density in the air gap (T),
l is the length of voice coil conductor in magnetic gap (m)

$$k_0 = \omega_1^2 \omega_2^2 \omega_3 \quad (38)$$

$$k_1 = \omega_1^2 \omega_2^2 + \omega_1 \omega_2 \omega_3 \left(\frac{\omega_1}{Q_2} + \frac{\omega_2}{Q_1}\right) \quad (39)$$

$$k_2 = \frac{\omega_1 \omega_2^2}{Q_1} + \frac{\omega_2 \omega_1^2}{Q_2} + \omega_3\left(\omega_1^2 + \omega_2^2\right) + \frac{\omega_1 \omega_2 \omega_3}{Q_1 Q_2} \quad (40)$$

$$k_3 = \omega_1^2 + \omega_2^2 + \frac{\omega_1 \omega_2}{Q_1 Q_2} + \frac{\omega_1 \omega_3}{Q_1} + \frac{\omega_2 \omega_3}{Q_2} \quad (41)$$

$$k_4 = \frac{\omega_1}{Q_1} + \frac{\omega_2}{Q_2} + \omega_3 \quad (42)$$

The denominator polynomial in s can be tailored to produce a standard filter frequency-response shape. The resonant frequencies (ω_1, ω_2, ω_3) and their associated Q values are calculated from the real and imaginary parts of the root loci on the complex plane as follows

$$\omega_1 = \frac{1}{\sqrt{\alpha_1^2 + \beta_1^2}} \quad (43)$$

$$\omega_2 = \frac{1}{\sqrt{\alpha_2^2 + \beta_2^2}} \quad (44)$$

$$\omega_3 = \frac{1}{\alpha_3} \quad (45)$$

$$Q_1 = \frac{\sqrt{\alpha_1^2 + \beta_1^2}}{2\alpha_1} \quad (46)$$

$$Q_2 = \frac{\sqrt{\alpha_2^2 + \beta_2^2}}{2\alpha_2} \quad (47)$$

where α_1, α_2 & α_3 are the real parts and β_1, β_2 & β_3 are the imaginary parts of the root loci. These are given for a selection of frequency response shapes in Table 13.

Frequency Response Shape	α_1	β_1	α_2	β_2	α_3	ω_1	Q_1	ω_2	Q_2	ω_3
Synchronous	2.59327	0.00000	2.59327	0.00000	2.59327	0.38561	0.50000	0.38561	0.50000	0.38561
Bessel	1.38510	0.72010	0.96060	1.47560	1.50690	0.64057	0.56353	0.56795	0.91647	0.66361
B5 (Butterworth)	0.80902	0.58779	0.30902	0.95106	1.00000	0.99999	0.61803	1.00000	1.61803	1.00000
0.01dB Ripple Chebyshev	0.51199	0.58787	0.19556	0.95120	0.63285	1.28277	0.76131	1.02977	2.48283	1.58015
0.1dB Ripple Chebyshev	0.38423	0.58843	0.14676	0.95211	0.47493	1.42294	0.91452	1.03804	3.28201	2.10556
0.25dB Ripple Chebyshev	0.32469	0.58917	0.12402	0.95330	0.40134	1.48650	1.03593	1.04022	3.87568	2.49164
0.5dB Ripple Chebyshev	0.27672	0.59020	0.10570	0.95497	0.34205	1.53408	1.17781	1.04080	4.54496	2.92355

Table 13. Root Loci for a selection of 5th-Order Frequency Response Shapes

7 VENTED-BOX SYSTEM ALIGNMENTS WITH 1ST-ORDER ISOLATED FILTER

A vented-box system with a 1st-order isolated filter shown in Fig. 18. The actual transfer function that relates the sound pressure $p(r)$ at a distance r in free space for a given voltage e_{in} at the input of the filter is given by

$$p(r) = \frac{\left(\frac{A\rho_0 S_D B l}{4\pi r M_{MD}(R_E + R_S)}\right) s^5 e_{in}}{\left\{s^4 + \left(\frac{\omega_S}{Q_{ES}} + \frac{\omega_B}{Q_L}\right)s^3 + \left[\left(1 + \frac{V_{AS}}{V_B}\right)\omega_S^2 + \omega_B^2 + \frac{\omega_S \omega_B}{Q_{ES} Q_L}\right]s^2 + \omega_S \omega_B \left(\frac{\omega_S}{Q_L} + \frac{\omega_B}{Q_{ES}}\right)s + \omega_S^2 \omega_B^2\right\}\left(s^2 + \omega_E\right)} \quad (48)$$

The normalised rms diaphragm displacement is given by

$$\frac{x}{x_{DC}} = \frac{\omega_S^2\left(s^2 + \frac{\omega_B}{Q_L}s + \omega_B^2\right)s}{\left\{s^4 + \left(\frac{\omega_S}{Q_{ES}} + \frac{\omega_B}{Q_L}\right)s^3 + \left[\left(1 + \frac{V_{AS}}{V_B}\right)\omega_S^2 + \omega_B^2 + \frac{\omega_S \omega_B}{Q_{ES} Q_L}\right]s^2 + \omega_S \omega_B \left(\frac{\omega_S}{Q_L} + \frac{\omega_B}{Q_{ES}}\right)s + \omega_S^2 \omega_B^2\right\}\left(s^2 + \omega_E\right)} \quad (49)$$

Equating the polynomial coefficients of the two transfer functions, given by Eqs. (36) & (48), yields a set of five simultaneous equations. Solving these equations gives us the five following Eqs. (50) to (54) that are used to generate each alignment from the root loci

$$\frac{\omega_B^4}{Q_L} - \left(\frac{\omega_1}{Q_1} + \frac{\omega_2}{Q_2}\right)\omega_B^3 + \omega_1\,\omega_2\left(\frac{\omega_1}{Q_2} + \frac{\omega_2}{Q_1}\right)\omega_B - \frac{\omega_1^2\,\omega_2^2}{Q_L} = 0 \tag{50}$$

Eq. (50) above is solved for ω_B. Although this is a 4th-order polynomial with four roots, only one is positive and real.

$$\omega_S = \frac{\omega_1\,\omega_2}{\omega_B} \tag{51}$$

$$Q_{ES} = \frac{\omega_S}{\frac{\omega_1}{Q_1} + \frac{\omega_2}{Q_2} - \frac{\omega_B}{Q_L}} \tag{52}$$

$$\frac{V_{AS}}{V_B} = \frac{1}{\omega_S^2}\left(\omega_1^2 + \omega_2^2 + \frac{\omega_1\,\omega_2}{Q_1\,Q_2} - \omega_B^2 - \frac{\omega_S\,\omega_B}{Q_{ES}\,Q_L}\right) - 1 \tag{53}$$

$$\omega_E = \omega_3 \tag{54}$$

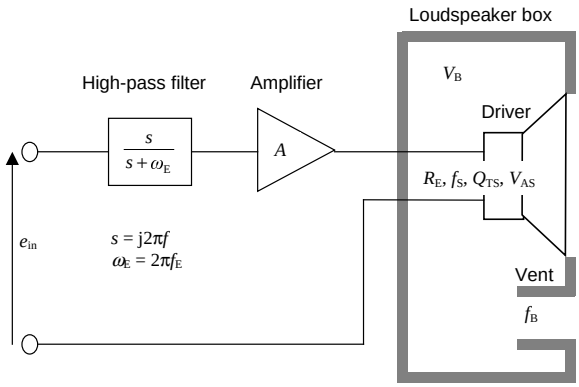

Fig. 18. Vented-box system with 1st-order isolated filter

Response shape	f_3/f_S	V_{AS}/V_B	Q_{TS}	f_E/f_S	f_B/f_S
Synchronous	2.5933	3.4490	0.2593	1.0000	1.0000
Bessel	1.6317	1.5112	0.3666	1.0828	0.9687
Butterworth	1.0000	0.7010	0.4777	1.0000	1.0000
0.01dB Cheby	0.8115	0.2891	0.6331	1.2823	0.8699
0.1dB Cheby	0.7362	0.1627	0.7911	1.5502	0.8006
0.25dB Cheby	0.7035	0.1150	0.9183	1.7529	0.7653
0.5dB Cheby	0.6780	0.0803	1.0713	1.9821	0.7339

Table 14. Alignments for lossy vented-box system with isolated 1st-order high-pass filter

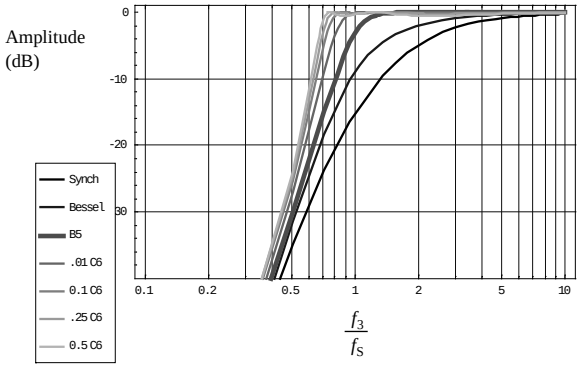

Fig. 19. Amplitude vs frequency plots for lossy vented-box system with isolated 1st-order high-pass filter

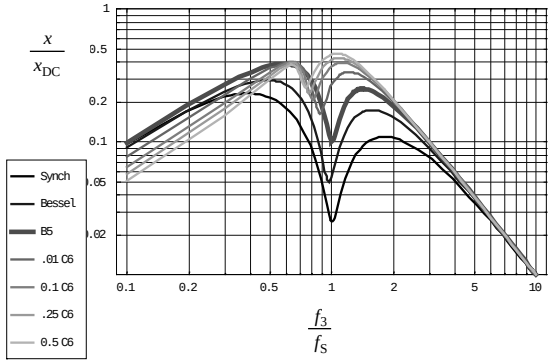

Fig. 20. Displacement vs frequency plots for lossy vented-box system with isolated 1st-order high-pass filter

8 VENTED-BOX SYSTEM ALIGNMENTS WITH 1ST-ORDER NON-ISOLATED FILTER

A vented-box system with a 1st-order non-isolated filter shown in Figs. 21 and 22. The actual transfer function that relates the sound pressure $p(r)$ at a distance r in free space for a given voltage e_{in} at the input of the filter is given by

$$p(r) = \frac{\left(\frac{A\,\rho_0\,S_D\,B\,l}{4\pi\,r\,M_{MD}\,(R_E + R_S)}\right)s^5\,e_{in}}{s^5 + \left(\frac{\omega_S}{Q_{ES}} + \frac{\omega_B}{Q_L} + \omega_E\right)s^4 + \left[\left(1 + \frac{V_{AS}}{V_B}\right)\omega_S^2 + \omega_B^2 + \frac{\omega_S\,\omega_B}{Q_{ES}Q_L} + \frac{\omega_B\,\omega_E}{Q_L}\right]s^3 + \left[\omega_S^2\left\{\frac{\omega_B}{Q_L} + \left(1 + \frac{V_{AS}}{V_B}\right)\omega_E\right\} + \omega_B^2\left(\frac{\omega_S}{Q_{ES}} + \omega_E\right)\right]s^2 + \omega_S^2\,\omega_B\left(\omega_B + \frac{\omega_E}{Q_L}\right)s + \omega_S^2\,\omega_B^2\,\omega_E} \tag{55}$$

The normalised rms diaphragm displacement is given by

$$\frac{x}{x_{DC}} = \frac{\omega_S^2\left(s^2 + \frac{\omega_B}{Q_L}s + \omega_B^2\right)s}{s^5 + \left(\frac{\omega_S}{Q_{ES}} + \frac{\omega_B}{Q_L} + \omega_E\right)s^4 + \left[\left(1 + \frac{V_{AS}}{V_B}\right)\omega_S^2 + \omega_B^2 + \frac{\omega_S\omega_B}{Q_{ES}Q_L} + \frac{\omega_B\omega_E}{Q_L}\right]s^3 + \left[\omega_S^2\left\{\frac{\omega_B}{Q_L} + \left(1 + \frac{V_{AS}}{V_B}\right)\omega_E\right\} + \omega_B^2\left(\frac{\omega_S}{Q_{ES}} + \omega_E\right)\right]s^2 + \omega_S^2\omega_B\left(\omega_B + \frac{\omega_E}{Q_L}\right)s + \omega_S^2\omega_B^2\omega_E} \quad (56)$$

Equating the polynomial coefficients of the two transfer functions, given by Eqs. (37) & (55), yields a set of five simultaneous equations. Solving these equations gives us the five following Eqs. (57) to (61) that are used to generate each alignment from the root loci

$$k_1 Q_L^2 \omega_B^6 + Q_L\left[(k_0 - k_1 k_4)Q_L^2 - 2k_0\right]\omega_B^5 + 2k_0 k_4 Q_L^2 \omega_B^4 + Q_L^3(k_1 k_2 - k_0 k_3)\omega_B^3 - Q_L^2\left(k_1^2 + k_0 k_2\right)\omega_B^2 + 2k_0 k_1 Q_L \omega_B - k_0^2 = 0 \quad (57)$$

Eq. (57) above is solved for ω_B. Although this is a 6th-order polynomial with six roots, only one is positive and real.

$$\omega_E = -\frac{k_0\,\omega_B}{\frac{k_0}{Q_L} - k_1\,\omega_B} \quad (58)$$

$$\omega_S = \frac{1}{\omega_B}\sqrt{\frac{k_0}{\omega_E}} \quad (59)$$

$$Q_{ES} = \frac{\omega_S}{k_4 - \frac{\omega_B}{Q_L} - \omega_E} \quad (60)$$

$$\frac{V_{AS}}{V_B} = \frac{1}{\omega_S^2}\left\{k_3 - \left[\left(1 - \frac{1}{Q_L^2}\right)\omega_B + \frac{k_4}{Q_L}\right]\omega_B\right\} - 1 \quad (61)$$

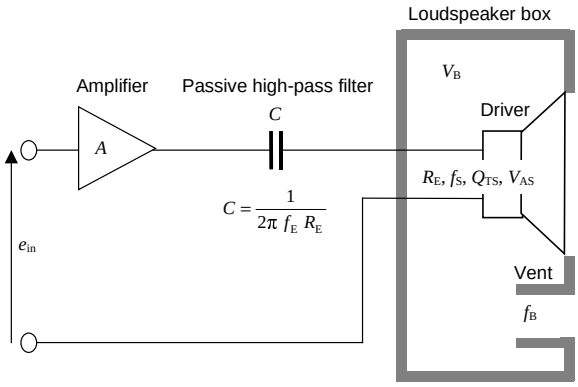

Fig. 21. Vented-box system with passive 1st-order non-isolated filter

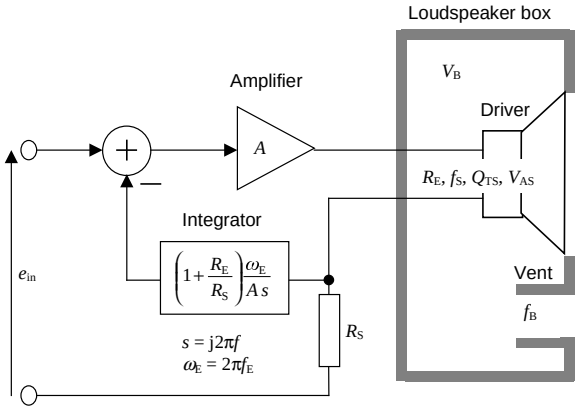

Fig. 22. Vented-box system with active 1st-order non-isolated filter

Response shape	f_3/f_S	V_{AS}/V_B	Q_{TS}	f_E/f_S	f_B/f_S
Synchronous	1.5047	1.5153	0.3737	0.1187	0.7444
Bessel	0.9730	0.7707	0.4775	0.1623	0.6870
Butterworth	0.6207	0.3709	0.5842	0.1999	0.6789
0.01dB Cheby	0.5018	0.2102	0.6654	0.2608	0.5800
0.1dB Cheby	0.4567	0.1572	0.7053	0.3230	0.5317
0.25dB Cheby	0.4382	0.1345	0.7180	0.3727	0.5081
0.5dB Cheby	0.4243	0.1146	0.7200	0.4319	0.4873

Table 15. Alignments for lossy vented-box system with non-isolated 1st-order high-pass filter

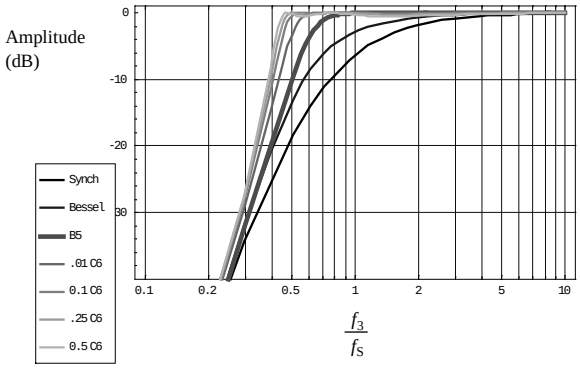

Fig. 23. Amplitude vs frequency plots for lossy vented-box system with non-isolated 1st-order high-pass filter

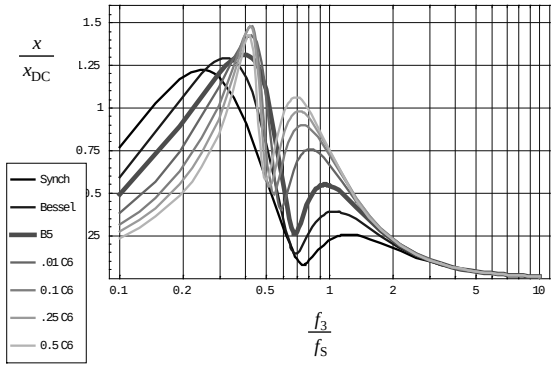

Fig. 24. Displacement vs frequency plots for lossy vented-box system with non-isolated 1st-order high-pass filter

9 1ST-ORDER LEMF

A lossy vented-box system with a 1st-order LEMF is shown in Fig. 25. The actual transfer function that relates the sound pressure $p(r)$ at a distance r in free space for a given voltage e_{in} at the input of the filter is given by

$$p(r) = \frac{\left(\frac{s+\omega_Z}{s+\omega_F}\right)\left(\frac{A\rho_0 S_D Bl}{4\pi r M_{MD}\left(R_E+R_S\right)}\right)s^5 e_{in}}{s^5+\left(\frac{\omega_S}{Q_{ES}}+\frac{\omega_B}{Q_L}+\omega_E\right)s^4+\left[\left(1+\frac{V_{AS}}{V_B}\right)\omega_S^2+\omega_B^2+\frac{\omega_S\omega_B}{Q_{ES}Q_L}+\frac{\omega_B\omega_E}{Q_L}\right]s^3+\left[\omega_S^2\left\{\frac{\omega_B}{Q_L}+\left(1+\frac{V_{AS}}{V_B}\right)\omega_E\right\}+\omega_B^2\left(\frac{\omega_S}{Q_{ES}}+\omega_E\right)\right]s^2+\omega_S^2\omega_B\left(\omega_B+\frac{\omega_E}{Q_L}\right)s+\omega_S^2\omega_B^2\omega_E} \quad (62)$$

A generic 6th-order high-pass system transfer-function that relates the sound pressure $p(r)$ at a distance r in free space for a given voltage e_{in} at the input of the LEMF is given by

$$p(r) = \frac{\left(\frac{s+\omega_Z}{s+\omega_3}\right)\left(\frac{\rho_0 S_D Bl}{4\pi r M_{MD}\left(R_E+R_S\right)}\right)s^5 e_{in}}{\left(s^2+\frac{\omega_1}{Q_1}s+\omega_1^2\right)\left(s^2+\frac{\omega_2}{Q_2}s+\omega_2^2\right)\left(s+\omega_Z\right)} \quad (63)$$

$$= \frac{\left(\frac{A\rho_0 S_D Bl}{4\pi r M_{MD}\left(R_E+R_S\right)}\right)s^6 e_{in}}{s^5+k_4 s^4+k_3 s^3+k_2 s^2+k_1 s+k_0} \quad (64)$$

where

$$k_0 = \omega_1^2\,\omega_2^2\,\omega_Z \quad (65)$$

$$k_1 = \omega_1^2\,\omega_2^2+\omega_1\,\omega_2\,\omega_Z\left(\frac{\omega_1}{Q_2}+\frac{\omega_2}{Q_1}\right) \quad (66)$$

$$k_2 = \frac{\omega_1\,\omega_2^2}{Q_1}+\frac{\omega_2\,\omega_1^2}{Q_2}+\omega_Z\left(\omega_1^2+\omega_2^2\right)+\frac{\omega_1\,\omega_2\,\omega_Z}{Q_1\,Q_2} \quad (67)$$

$$k_3 = \omega_1^2+\omega_2^2+\frac{\omega_1\,\omega_2}{Q_1\,Q_2}+\omega_Z\left(\frac{\omega_1}{Q_1}+\frac{\omega_2}{Q_2}\right) \quad (68)$$

$$k_4 = \frac{\omega_1}{Q_1}+\frac{\omega_2}{Q_2}+\omega_Z \quad (69)$$

It can be seen that the $(s+\omega_Z)$ terms in the numerator and denominator of Eq. (63) cancel. Equating the polynomial coefficients of the two transfer functions, given by Eqs. (62) & (64), yields a set of five simultaneous equations. Solving these equations gives us the five following Eqs. (70) to (74) that are used to generate each alignment from the root loci

$$k_1\,Q_L^2\,\omega_B^6+Q_L\left[\left(k_0-k_1\,k_4\right)Q_L^2-2k_0\right]\omega_B^5+2k_0\,k_4\,Q_L^2\,\omega_B^4 +Q_L^3\left(k_1\,k_2-k_0\,k_3\right)\omega_B^3-Q_L^2\left(k_1^2+k_0\,k_2\right)\omega_B^2+2k_0\,k_1\,Q_L\,\omega_B-k_0^2 =0 \quad (70)$$

Eq. (70) above is solved for ω_B. Although this is a 6th-order polynomial with six roots, only one is positive and real.

$$\omega_E = -\frac{k_0\,\omega_B}{\frac{k_0}{Q_L}-k_1\,\omega_B} \quad (71)$$

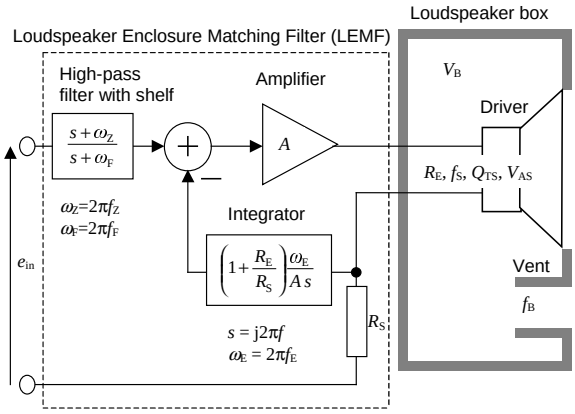

Fig. 25. Vented-box system with 1st-order LEMF

$$\omega_S = \frac{\sqrt{k_0}}{\omega_B\sqrt{\omega_E}} \quad (72)$$

$$Q_{ES} = \frac{\omega_S}{k_4-\frac{\omega_B}{Q_L}-\omega_E} \quad (73)$$

$$\frac{V_{AS}}{V_B} = \frac{1}{\omega_S^2}\left\{k_3-\left[\left(1-\frac{1}{Q_L^2}\right)\omega_B+\frac{k_4}{Q_L}\right]\omega_B\right\}-1 \quad (74)$$

These are essentially the same equations as for the non-isolated filter but with ω_3 replaced by ω_Z where;

$$0 \le \omega_Z \le \omega_3 \quad (75)$$

and

$$\omega_F = \omega_3 \quad (76)$$

By varying the shelf frequency ω_Z from dc up to ω_F, a range of solutions is obtained from isolated (ω_Z=0) to non-isolated (ω_Z=ω_F). Hence

$$0 \le \frac{\omega_Z}{\omega_F} \le 1 \quad (77)$$

The last Eq. (78) forms a parameter that becomes the basis of the alignment charts for a 1st-order LEMF as shown in Tables 16, 17 & 18.

f_Z/f_F	f_3/f_S	V_{AS}/V_B	Q_{TS}	f_Z/f_S	f_F/f_S	f_E/f_S	f_B/f_S
1.00	Bessel Alignment with Non-Isolated Filter						
	0.973	0.771	0.478	0.646	0.646	0.162	0.687
0.80	1.023	0.767	0.481	0.543	0.679	0.161	0.700
0.60	1.088	0.783	0.479	0.433	0.722	0.156	0.718
0.40	1.179	0.843	0.469	0.313	0.782	0.143	0.747
0.30	1.242	0.906	0.457	0.247	0.824	0.131	0.771
0.20	1.325	1.009	0.439	0.176	0.880	0.111	0.806
0.15	1.379	1.085	0.426	0.137	0.915	0.095	0.831
0.10	1.445	1.186	0.411	0.096	0.959	0.074	0.864
0.05	1.526	1.323	0.391	0.051	1.013	0.044	0.908
0.00	Bessel Alignment with Isolated Filter						
	1.632	1.511	0.367	0.000	1.083	0.000	0.969

Table 16. Bessel (Be5) alignments for lossy vented-box system with 1st-order LEMF

f_Z/f_F	f_3/f_S	V_{AS}/V_B	Q_{TS}	f_Z/f_S	f_F/f_S	f_E/f_S	f_B/f_S
1.00	B5 Alignment with Non-Isolated Filter						
	0.621	0.371	0.584	0.621	0.621	0.200	0.679
0.80	0.656	0.374	0.590	0.525	0.656	0.196	0.705
0.60	0.700	0.388	0.590	0.420	0.700	0.186	0.738
0.40	0.760	0.425	0.579	0.304	0.760	0.165	0.784
0.30	0.799	0.458	0.567	0.240	0.799	0.147	0.815
0.20	0.848	0.508	0.548	0.170	0.848	0.120	0.857
0.15	0.878	0.542	0.535	0.132	0.878	0.100	0.884
0.10	0.912	0.583	0.520	0.091	0.912	0.075	0.915
0.05	0.952	0.636	0.501	0.048	0.952	0.043	0.953
0.00	B5 Alignment with Isolated Filter						
	1.000	0.701	0.478	0.000	1.000	0.000	1.000

Table 17. Butterworth (B5) alignments for lossy vented-box system with 1st-order LEMF

f_Z/f_F	f_3/f_S	V_{AS}/V_B	Q_{TS}	f_Z/f_S	f_F/f_S	f_E/f_S	f_B/f_S
1.00	0.01dB Chebyshev Alignment with Non-Isolated Filter						
	0.502	0.210	0.665	0.793	0.793	0.261	0.580
0.80	0.532	0.200	0.691	0.673	0.841	0.256	0.607
0.60	0.570	0.194	0.713	0.540	0.901	0.243	0.640
0.40	0.620	0.195	0.725	0.392	0.979	0.216	0.683
0.30	0.652	0.202	0.723	0.309	1.030	0.192	0.711
0.20	0.691	0.217	0.711	0.218	1.092	0.155	0.748
0.15	0.715	0.228	0.699	0.169	1.130	0.130	0.771
0.10	0.742	0.243	0.683	0.117	1.173	0.098	0.798
0.05	0.774	0.263	0.661	0.061	1.223	0.056	0.830
0.00	0.01dB Chebyshev Alignment with Isolated Filter						
	0.812	0.289	0.633	0.000	1.282	0.000	0.870

Table 18. 0.01dB Chebyshev (C5) alignments for lossy vented-box system with 1st-order LEMF

10 CONCLUSIONS

In this paper, a range of lossy isolated and non-isolated filter-assisted vented-box system alignments have been presented together with their associated amplitude and displacement plots. This enabled us to select some key frequency-response shapes for which LEMF alignments were derived as alternatives to the Butterworth LEMF alignments presented in Part I. Lossy 5th-order LEMF alignments were derived for these frequency response shapes corresponding to a Q_L value of 7. In the case of 6th-order LEMF alignments, the lossy equations are virtually impossible to solve and so loss-less alignments are given together with correction factors derived for the isolated and non-isolated filter assisted alignments at the extremes of the LEMF range.

From Fig. 26 below, it can be seen how the loss-less 6th-order alignments derived in Parts I and II of this paper fit into the three-way efficiency/bandwidth/size trade-off. This relationship can be approximated by the formula

$$(Power\ Lift)\left(\frac{V_B}{V_{AS}}\right)^2\left(\frac{f_3}{f_S}\right)^4 \approx 0.5$$

The choice of alignment depends entirely upon the application and the type of driver to be used and the most useful are probably those that lie inside the triangle or within its immediate vicinity. Alignments outside this region would result in designs that are either extremely large, very power hungry or severely band limited. The B6 Class II alignment appears to be a useful hub at the centre as its f_3/f_S and V_B/V_S values are both unity and the power lift (or rather power cut in this case) is 0.5, which means that the input power is halved at f_3 when the acoustic output power is also halved. The alignments can be classified briefly as follows: -

- **Low Power.** For portable equipment, where power consumption is a concern, the C6 Type 3 to Class III alignments appear to be the most efficient providing the box volume is available.

- **Small size.** If small box size is the main requirement, then the Type 2 to Class I ranges provide a fair amount of flexibility providing the speaker and amplifier have sufficient power ratings. The Chebyshev alignments provide an extended low-frequency response at the cost of high power assistance whereas the Bessel alignments have a higher cut-off frequency but with an easier drive requirement. The $B3^2$ alignments provide a particularly useful range.

- **Maximum low-frequency extension.** If maximum low-frequency extension is desired, then the Type 1 to Class II ranges are of particular interest. Here, the extra bandwidth is obtained through a moderate amount of power lift together with an increase in the box volume. Unfortunately, the displacement curve is non-symmetrical with greater excursion below the box resonance than above and so this arrangement is best suited to long-throw drivers. The problem can be avoided if the speaker is to be used in an application where it can be arranged for the programme material to be mainly above f_B, such as a musical instrument or MIDI player. Here, the asymmetry is positively beneficial since it minimises the pass-band displacement.

Interestingly, the Q_{EN} value for the range of LEMF alignments that lie between Class II and Class III isolated is consistently very high (greater than 25), with the exception of Chebyshev where this range does not exist. This implies that here the amount of current feedback is minimal and therefore this range could be closely approximated simply by using an isolated filter with no LEMF arrangement at all. Obviously, these alignments have always existed, but they do not appear to have been known about. The $B3^2$ Class II to Class III negligible-feedback alignments appear to give the most useful range of box volumes with V_B/V_{AS} varying from 0.5 to 1.0, and could even be extended down to 0.36 in the Type 1 to Class I/II range where Q_{EN} is still very high. The least useful Class II to Class III negligible-feedback range is that of the Bessel alignments, which only provide a 17% variation in volume.

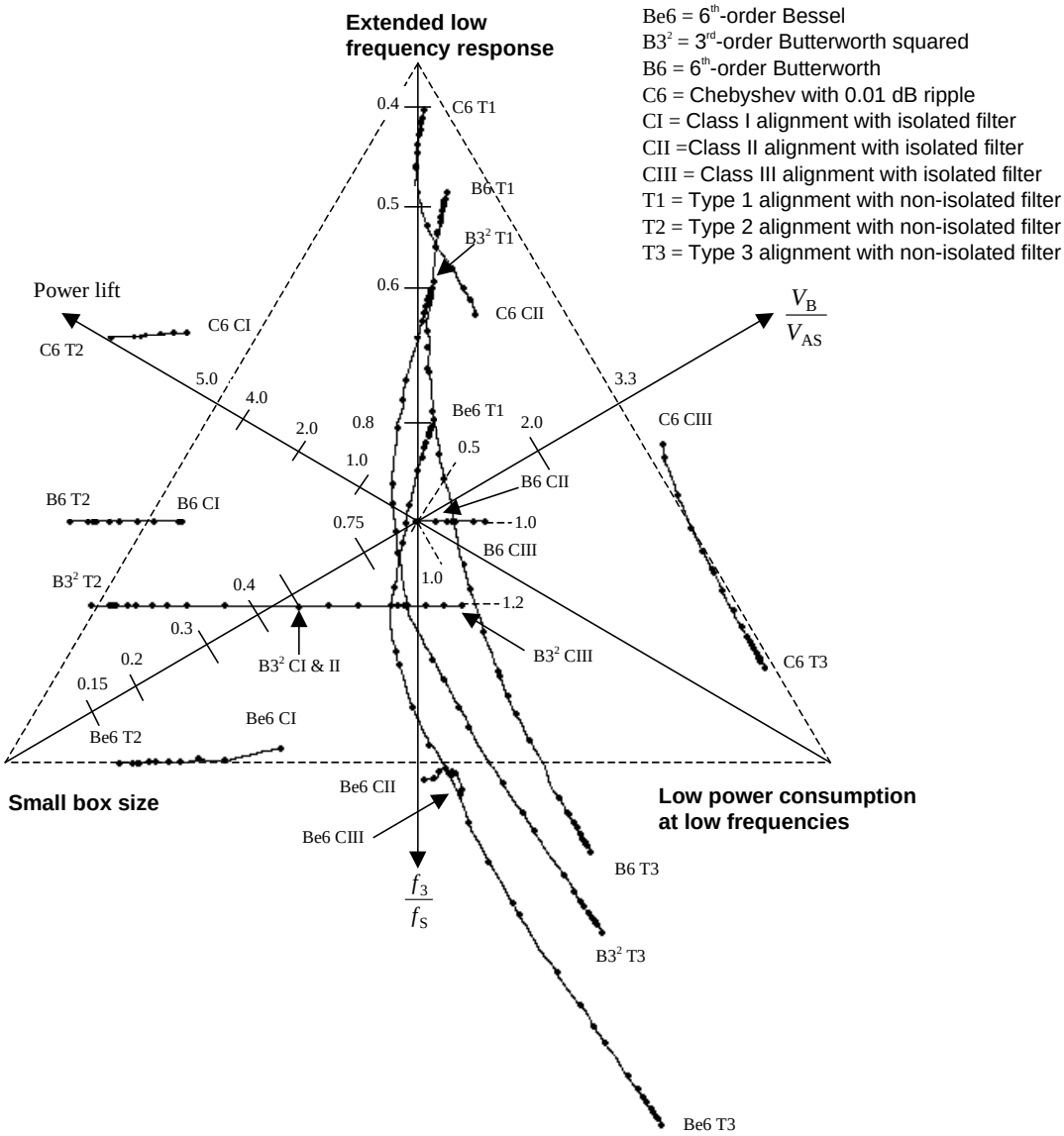

Figure 26. Loudspeaker triangle for loss-less 6th order LEMF alignments

Whichever alignments are selected, the following rules of thumb apply: -

- A larger box allows greater maximum SPL at low frequencies before the power limit is reached.
- A well optimised design is achieved if the coil travel limit coincides with the input power limit.
- For a given box size, the low-frequency response can be extended by increasing the input power. However, depending upon the bass content of the programme material, this can increase the risk of premature power and/or travel limiting at low frequencies.

In conclusion, the LEMF scheme does appear to increase the flexibility of the vented-box system design process with regard to the matching of a driver to a particular box size. The whole process could be streamlined further by incorporating it into a suitable computer software application, as has been done with previous loudspeaker alignments.

11 ACKNOWLEDGMENT

The author wishes to express his gratitude to Noel Lobo for the valuable guidance he gave in the use of Mathematica for solving the equations. Thanks are also due to Trevor Dragwidge, Brian Griffiths, Benedict Slotte, Andrew Bright and Juha Backman for their encouragement and support.

12 REFERENCES

[1] R. A. R. Bywater and H. J. Wiebell, "Alignment of Filter-Assisted Vented-Box Loudspeaker Systems with Enclosure Losses," in *Loudspeakers—An Anthology*, vol. 2 (Audio Engineering Society, New York, 1984), pp. 310–321.

[2] A. I. Zverev, *Handbook of Filter Synthesis* (John Wiley and Sons, Inc., New York, 1967)